

Graphene Quantum Dots as Fluorescence Probes for Turn-off Sensing of Melamine in the Presence of Hg^{2+}

Lingling Li,^{†,§} Gehui Wu,^{†,§} Tao Hong,[†] Zhouyang Yin,[†] Dong Sun,[†] E. S. Abdel-Halim,[‡] and Jun-Jie Zhu^{*,†}

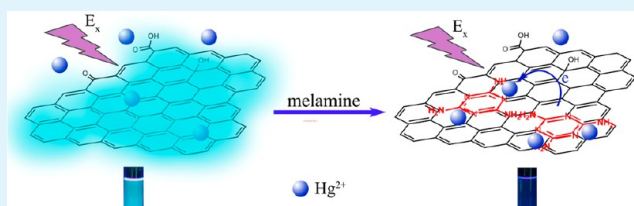
[†]State Key Laboratory of Analytical Chemistry for Life Science, School of Chemistry and Chemical Engineering, Nanjing University, Nanjing 210093, China

[‡]Petrochemical Research Chair, Department of Chemistry, College of Science, King Saud University, Riyadh 11451, P. O. Box 2455, Kingdom of Saudi Arabia

S Supporting Information

ABSTRACT: A rapid and sensitive fluorescence sensing system for melamine based on charge transfer quenching of the fluorescence of graphene quantum dots (GQDs) in the presence of Hg^{2+} is proposed. The synthesized GQDs were strongly luminescent with predominantly aromatic sp^2 domains. Melamine could coordinate with mercury through nitrogen atoms in both its amine and triazine groups and bring more Hg^{2+} to the surface of GQDs through π - π stacking, thus leading to quenching of the GQDs' fluorescence. The quenching mechanism was investigated in detail and ascribed to charge transfer from the GQDs to Hg^{2+} with melamine acting as the linkage agent. The melamine demonstrated a linear range 0.15–20 μM and a detection limit of 0.12 μM , which was far below the regulatory level, suggesting the promising practical usage of this sensing system. This sensing system also possessed high selectivity for melamine in the presence of possible interferences. Finally, this novel sensor was successfully applied for melamine detection in raw milk and satisfactory recovery was achieved.

KEYWORDS: graphene quantum dots, melamine, mercury ions, charge transfer, fluorescence quenching, sensor



INTRODUCTION

Graphene quantum dots (GQDs), generally produced either from graphene-based precursors or via the rigorous synthetic chemistry of graphene-like smaller polycyclic aromatic hydrocarbon molecules (PAHs), are attracting growing interest for their applications in electronic and optical areas.^{1–4} Due to quantum confinement and edge effects, GQDs possess superior properties compared with those of larger sheets of graphene and graphene oxide (GO), such as a tunable band gap and high photoluminescence activity. To date, great effort has been devoted to the large-scale preparation of GQDs,^{5–8} and many reports have shown that GQDs have the potential to be employed in bioimaging, photocatalyst, and energy-related devices.^{9–11} One of the most fascinating features of GQDs is their fluorescence (FL), and various sizes of GQDs have low cytotoxicity and high photostability.^{12–14} However, the practical implementation of GQDs in sensing applications is still in its initial stages: only a few GQDs-based FL sensors working in “turn-off” or “turn-off-on” modes based on energy transfer, charge transfer or other mechanisms have been reported.^{15–17}

As a raw chemical material, monomeric melamine is commonly combined with formaldehyde to create a resin having both excellent thermal resistance and heat tolerance. However, due to a melamine-tainted milk scandal in 2008, melamine has attracted much concern from the viewpoint of

food safety.¹⁸ It has been reported that the reaction of melamine with cyanuric acid through hydrogen bonding leads to the formation of insoluble crystals in the kidneys, causing renal failure in animals and humans.¹⁹ These safety concerns have spurred the development of various detection methods for melamine, including gas chromatography/mass spectrometry (GC/MS), enzyme-linked immunosorbent assay (ELISA), surface enhanced Raman spectroscopy (SERS), and electrochemical and colorimetric sensing methods.^{20–25} However, both GC/MS and ELISA methods are time-consuming and can be performed only by highly trained operators and with expensive scientific instruments. As a lower-cost alternative, an electrochemical sensing system can provide excellent analytical sensitivity, but in order to use such a system to detect melamine, which is innately non-electroactive, a redox-active modification of melamine is required. Most of the colorimetric sensors developed for the detection of melamine are based on the triple hydrogen-bonding recognition between melamine and cyanuric acid or thymine, both of which require costly chemical modification with a specific acceptor moiety.^{25–27} Thus, there is an urgent demand for the development of a simple, low-cost, time-saving, sensitive, and reliable method to

Received: November 28, 2013

Accepted: January 24, 2014

Published: January 24, 2014

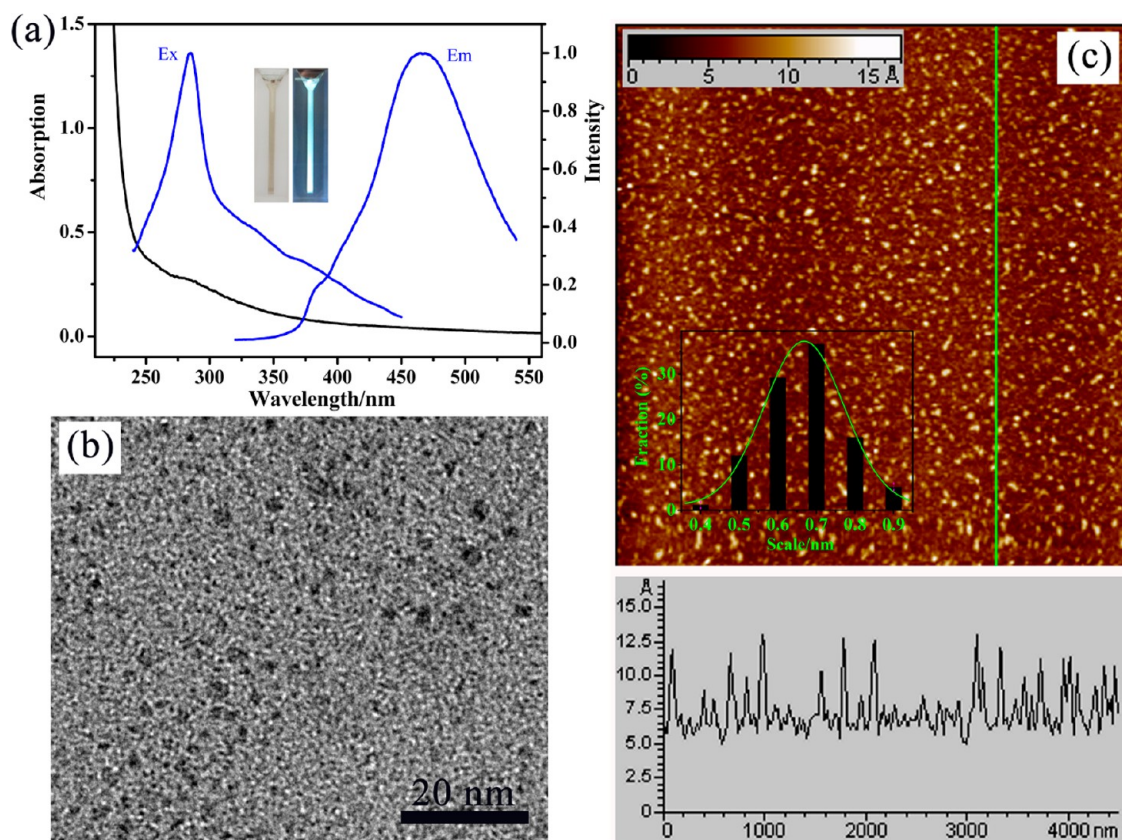


Figure 1. (a) UV-vis absorption (black) and FL excitation (Ex) and emission (Em) spectra of GQDs (blue). Insets were photographs of the GQDs aqueous solution taken under visible light and 365 nm UV light. (b) HRTEM image of GQDs. (c) AFM image and the corresponding height profile of GQDs. Inset shows the height distribution of the GQDs.

detect melamine. Fluorescence detection can be very fast, simple, and sensitive, and thus, FL analytical techniques are a promising alternative to monitor the concentration of melamine. Nevertheless, there are very few reports regarding the utilization of FL methods for melamine detection.²⁸

As a carbon-based nanomaterial, GQDs possess both sp^2 -bonded carbon lattices and surface functional groups (hydroxyl, carbonyl, and carboxylic acid groups), which facilitate grafting of other moieties to their surface through π - π stacking, electrostatic interaction, and chemical reactions. Metal ions (such as Hg^{2+} and Fe^{3+}) can bind with GQDs through surface functional groups or by means of surface adsorption and may quench the FL of GQDs.^{29,30} However, the metal ions' binding ability is highly dependent upon the degree of oxidation of the GQDs. More specifically, metal ions exhibit poor binding to reduced GQDs, and the corresponding FL quenching thus will also be decreased. On the other hand, it is expected that GQDs may have a certain affinity for melamine due to their π -conjugated structures, and melamine can coordinate with metal ions (such as Cu^{2+} and Ag^+).³¹ In this way, melamine may act as a linkage agent between GQDs and metal ions to bring them into proximity of each other, leading to the FL quenching of GQDs. We therefore hypothesized that it might be possible to use GQDs as a fluorescent probe for selective determination of melamine.

We report here a sensitive and selective method for melamine detection that is achieved by integrating the sp^2 -bonded carbon lattice structure and FL of GQDs with the unique structure of melamine (namely, its aromatic ring and amino groups). The FL quenching of GQDs was induced by

charge transfer between the GQDs and Hg^{2+} . To our knowledge, this is the first reported sensor for melamine detection based on the FL of GQDs.

EXPERIMENTAL SECTION

Materials and Apparatus. Graphite powder was purchased from J&K Scientific Ltd. $HgCl_2$ was obtained from Jiangsu Donggong Chemicals. Melamine was obtained from Shanghai Lingfeng Chemical Reagent Co., Ltd. Amino acids were purchased from Aladdin Industrial Corporation (Shanghai, China). All other reagents were of analytical reagent grade and used without further purification. Aqueous solutions were prepared with ultrapure water from an Elix 5 Pure Water System ($>18 M\Omega$ -cm, Millipore, U.S.A.).

Ultraviolet-visible (UV-vis) absorption spectra were obtained using a UV-3600 spectrophotometer (Shimadzu). FL spectra were obtained on a RF-5301PC spectrophotometer (Shimadzu, Kyoto, Japan). Fourier-transform infrared (FTIR) spectra were acquired on a Nicolet 6700 spectrophotometer (Nicolet, U.S.A.). X-ray diffraction (XRD) measurements were performed by an XRD-6000 powder diffractometer with $Cu K\alpha$ radiation (0.15418 nm) (Shimadzu, Japan). High-resolution transmission electron microscopy (HRTEM) images were taken using a JEOL 2010 electron microscope at an accelerating voltage of 200 kV. Atomic force microscopy (AFM) images were obtained in tapping mode using an Agilent 5500. The FL lifetime measurements were performed on an FLS920 time-resolved fluorescence spectrometer (Edinburgh Instruments). The microwave synthesis of GQDs was performed in a WBFY-201 microwave oven equipped with an atmospheric reflux device (Nanjing Keer Instrument Equipment Co. Ltd., Nanjing, China).

Synthesis of GQDs. Graphene oxide (GO) was synthesized from natural graphite powder by a modified Hummers method.³² Following the synthesis of GO, GQDs were synthesized according to a previous

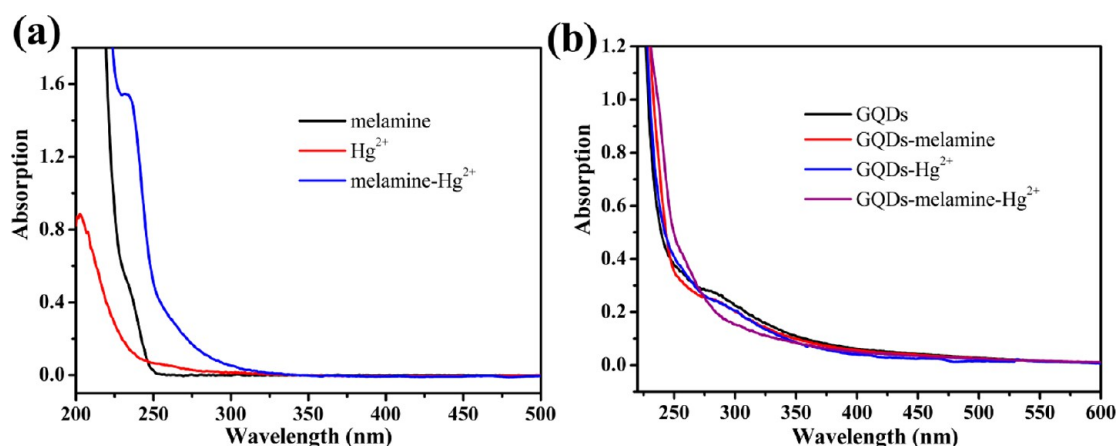


Figure 2. (a) UV-vis spectra of melamine (black), Hg²⁺ (red), and the Hg-melamine complex (blue) in aqueous solution. (b) UV-vis spectra of GQDs (black), GQDs-melamine (red), GQDs-Hg²⁺ (blue), and GQDs-melamine-Hg²⁺ (purple) in aqueous solution.

report with slight modifications.⁶ Briefly, GO solution (30 mL, 0.5 mg·mL⁻¹) was first mixed carefully with concentrated HNO₃ (8 mL) and H₂SO₄ (2 mL). Then, the mixture was heated and refluxed under microwave irradiation for 3 h in microwave oven operating at a power of 240 W. The product consisted of a brown transparent suspension and a black precipitate. After cooling to room temperature, the pH of the mixture was tuned to 8 with solid NaOH in an ice-bath. The suspension was filtered through a 0.22 μm microporous membrane to remove the large tracts of GO, and a deep yellow solution was obtained which was reduced with 1 g NaBH₄ under stirring at room temperature for 24 h. Then, HNO₃ solution was added dropwise to terminate the reaction, and the pH again was tuned to 8. The mixture was dialyzed in a dialysis bag (retained molecular weight: 1000 Da) to yield a solution of fluorescent GQDs.

Detection Procedure. Hg²⁺ is chosen as the metal ion for these experiments because it does not interfere with the FL of GQDs but can coordinate with melamine to form a complex. We observed that 40 μM Hg²⁺ induced a relatively small change to the FL intensity of GQDs, whereas huge quenching was observed in the presence of 40 μM of other metal ions (Cu²⁺, Pb²⁺, Co²⁺, Mn²⁺) (Figure S1 in the Supporting Information). Furthermore, Cd²⁺ and Ag⁺ had little influence on the FL intensity of GQDs both in the absence or presence of melamine, whereas the addition of Hg²⁺ with melamine led to FL quenching of GQDs. Therefore, Hg²⁺ was determined to be the most appropriate metal ion for these studies, and different amounts of melamine were titrated into the GQDs and Hg²⁺ mixed solution.

The typical assay procedure was as follows: 40 μL of HgCl₂ solution (1 mM) was mixed with 1 mL of GQDs stock solution (20 μg mL⁻¹). Then, melamine was added at various prescribed concentrations, and the mixture was incubated for 10 min at room temperature. The FL spectra were recorded by excitation with a wavelength of 285 nm.

Pretreatment of Milk Samples. Raw milk (1 g) spiked with a certain amount of melamine (0, 2.0, 8.0, or 20 mg for samples 1, 2, 3, and 4, respectively) was first mixed with 15 mL of 61 mM trichloroacetic acid and 5 mL of acetonitrile. After 15 min sonication and 10 min shaking, the mixture was centrifuged at 9500 rpm for 10 min to separate the deposit. The supernatant was filtered through a 0.45 μm polytetrafluoroethylene filter membrane. The filtrate was adjusted to pH 7.0 with 1 M NaOH solution and diluted with water to 100 mL to obtain the samples for detection.

RESULTS AND DISCUSSION

Characterization of GQDs. In order to restore the sp²-bonded carbon network and increase the FL intensity, NaBH₄ was used as a reductant. In the FTIR spectrum (Figure S2 in the Supporting Information), the absorption band of C-OH at 1389 cm⁻¹ for GQDs was obviously enhanced compared with that of GQDs before reduction, suggesting the C=O moiety

was partly reduced. GQDs were functionalized with oxygen-containing groups including hydroxyl and alkoxy groups, which made them very soluble in water. GQDs showed a weak broad (002) peak centered at around 25.9 degrees (Figure S3 in the Supporting Information). The interlayer spacing is 0.344 nm, and the disappearance of the peak at 9.8 degrees indicates the reduction of oxygen functional groups between interlayers. The obtained GQDs showed a yellow color under visible light and emitted bright blue FL under UV light with a quantum yield of 15.1% (Table S1 in the Supporting Information). As shown in the FL spectra (Figure 1a), GQDs had optimal maximum excitation and emission wavelengths at 285 nm and 466 nm, respectively. A typical absorption peak at ca. 285 nm was observed in the UV-vis spectra of the GQDs, corresponding to the maximum excitation wavelength. This absorption could be assigned to the π-π* transition of aromatic sp² domains.³³ GQDs showed good photostability and the photoluminescence properties and appearance of GQDs in the presence of Hg²⁺ remained unchanged for three months in the air at room temperature. Figure 1b shows a representative high-resolution transmission electron microscope (HRTEM) image of the GQDs. The diameters of the GQDs were mainly distributed in the range 2–7 nm with an average diameter of 4.5 nm. The topographic heights of GQDs deposited on a mica substrate were studied by atomic force microscopy (AFM), and the results are shown in Figure 1c. The heights of the GQDs were mostly between 0.4 and 0.9 nm with an average height of 0.67 nm, indicating that most GQDs were single layered or bilayered, similar to those reported previously.^{1,8}

Coordination of Melamine with Hg²⁺. As can be seen in Figure S1 in the Supporting Information, melamine showed no FL when excited at 285 nm, and the addition of 15 μM of melamine induced no obvious change to the FL of GQDs. However, in the presence of 40 μM Hg²⁺, the addition of 15 μM of melamine resulted in a huge decrease of the FL intensity of the GQDs. It has been reported that a Hg-melamine complex forms in the presence of excess Hg²⁺.³¹ Thus, the interaction between melamine and mercury ions probably played an important role in the FL quenching of GQDs.

The coordination of melamine with Hg²⁺ was confirmed by the UV-vis spectra. Neither melamine nor Hg²⁺ solution showed obvious absorption at wavelengths longer than 250 nm (Figure 2a). In contrast, the strong absorption peak at 232 nm, observed when melamine was mixed with Hg²⁺, probably could

be attributed to the formation of a Hg–melamine complex. As shown in Figure 2b, the sole addition of melamine or Hg^{2+} into the GQDs solution caused little change to the UV–vis spectrum of GQDs. In contrast, the absorption peak at 285 nm blue-shifted to 260 nm upon addition of both melamine and Hg^{2+} , which further demonstrated the effect of coordination between melamine and Hg^{2+} . GQDs that were modified with the Hg–melamine complex exhibited a strong intermolecular interaction, leading to the blue-shift of the absorption peak. We also used FTIR spectroscopy to study this coordination effect. Three principal absorption regions (2800–3500, 1400–1650, and 800–1050 cm^{-1}) were observed in the FTIR spectrum of melamine (Figure 3). The 2800–3500 cm^{-1}

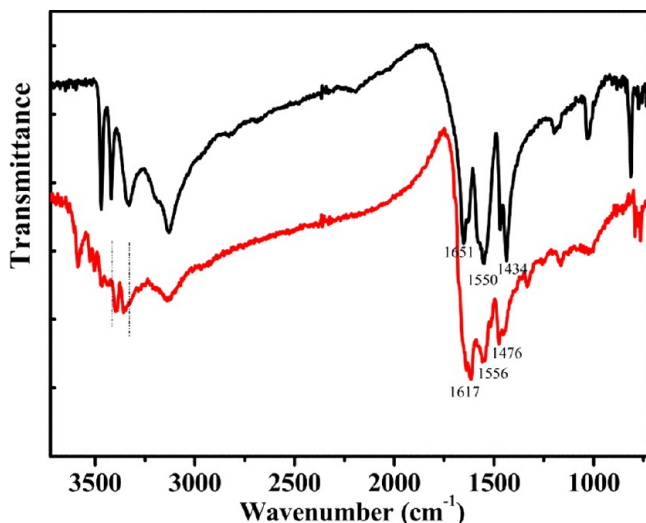


Figure 3. FTIR spectra of melamine (black) and of the Hg–melamine complex (red).

region encompassed the N–H stretching modes, and the two sharp high frequency bands (3469 and 3419 cm^{-1}) shifted closer to each other and became broader after reacting with Hg^{2+} . Some shifts were also observed in the ring distortion absorption region (1440–1650 cm^{-1}) upon formation of the Hg–melamine complex. Thus, changes in the N–H stretching and ring distortion absorption region suggested that coordination occurred through the amine nitrogen atoms together with those of triazine in melamine.³¹

Quenching Mechanism. The restored sp^2 -bonded carbon network of GQDs could serve as a substrate for anchoring aromatic molecules through π – π stacking.³⁴ The self-assembly of melamine on the surface of GQDs was confirmed by AFM. In addition to the above-mentioned heights of 0.4–0.9 nm observed for the as-prepared GQDs (Figure 1c), the GQDs–melamine complex exhibited an additional range of heights from 1.3 to 1.9 nm (Figure 4). This 1.3–1.9 nm height region was mainly due to the multiple noncovalent interactions between GQDs and melamine.

As shown in Figure 5b, GQDs possessed bright blue emission FL (vial 1 in Figure 5b) and still showed relatively strong emission in the presence of 2.0 ppm melamine (vial 2) or 40 μM Hg^{2+} (vial 3), respectively. However, upon addition of melamine (0.2, 0.8, 2.0 ppm melamine for vials 4, 5, 6, respectively) to the GQDs– Hg^{2+} solution, the FL of GQDs was largely quenched. We concluded that the combination of melamine and Hg^{2+} quenched the FL of the GQDs: melamine

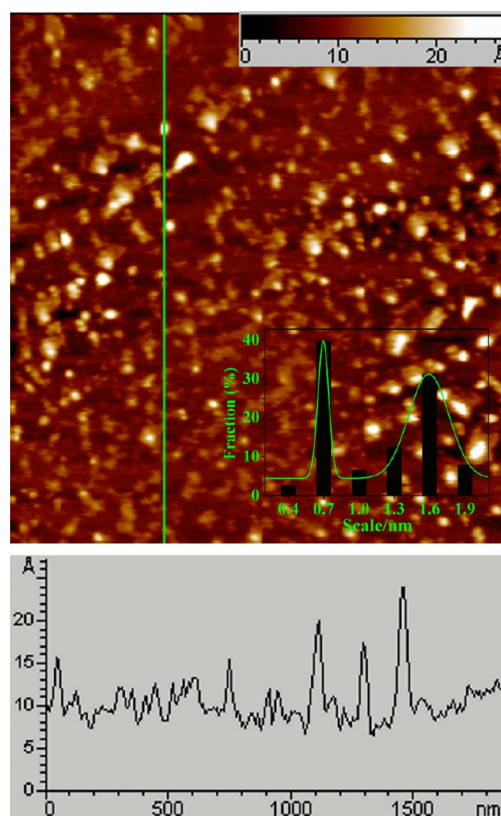


Figure 4. AFM image and corresponding height profile of GQDs in the presence of 4 μM melamine. Inset shows the height distribution of the GQDs.

coordinated with Hg^{2+} to form a Hg–melamine complex and attached on the surface of GQDs, which shortened the GQDs– Hg^{2+} distance. In contrast, in the absence of melamine, the distance between the GQDs and Hg^{2+} was relatively far, and thus charge transfer did not occur as substantially.

The AFM results shown above indicate that melamine could attach itself to the surface of the GQDs. Because melamine could also coordinate with Hg^{2+} , more free Hg^{2+} ions were in close proximity to the surface of GQDs through coordination with the Hg–melamine complex. The blue shift observed in the UV–vis spectrum of GQDs upon the addition of the Hg–melamine complex indicated a strong interaction between the GQDs and the attached complex. GQDs (the donor) and Hg^{2+} (the quencher) blended together, with melamine acting as a bridging agent. Energy transfer between the Hg–melamine complex and the GQDs does not adequately explain the observed FL quenching, because there is little overlap between the absorption spectrum of the Hg–melamine complex (Figure 2a) and the emission spectrum of the GQDs (Figure 1a).^{35,36} Thus, the FL quenching could be ascribed to charge transfer from the GQDs to Hg^{2+} in the presence of melamine, which served as the linkage between the two.

To verify our proposed quenching mechanism, we acquired time-resolved fluorescence spectra of the GQDs before and after addition of Hg^{2+} and melamine (Figure 6). The FL intensity decay curve of the GQDs could be fitted with a tri-exponential function, and three lifetimes (two fast components and a slow component) were obtained as listed in Table S2 in the Supporting Information. The slow component (τ_3) was suggested to be related to edge states of GQDs, and it increased from 21.39% to 44.95% after the addition of Hg^{2+} .³⁷ Oxygen-

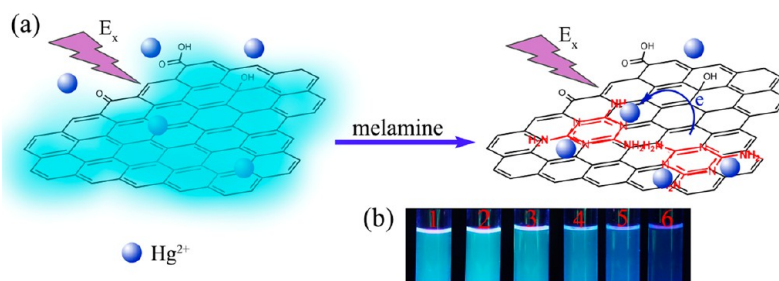


Figure 5. (a) Schematic illustration of melamine detection based on FL quenching of GQDs through charge transfer. (b) Optical photos of solutions of GQDs (vial 1) and GQDs in the presence of melamine (vial 2) or Hg^{2+} (vial 3), and of GQDs- Hg^{2+} in the presence of 0.2, 0.8, 2.0 ppm melamine for vials 4, 5, 6, respectively, taken under a 365 nm UV lamp.

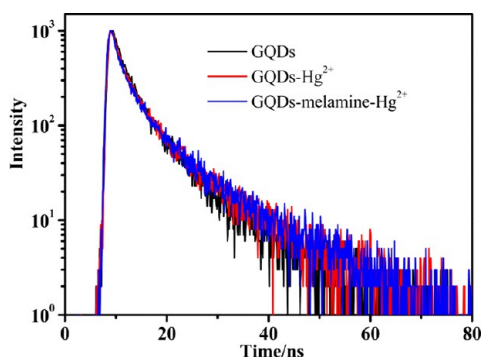


Figure 6. FL decay of GQDs at 466 nm as a function of time in the presence of Hg^{2+} and melamine.

containing groups (O—C=O, OH, and C=O groups) were mostly functioned at the edge of the GQDs, rather than the basal plane of the GQDs, and the binding of Hg^{2+} at the edge of the GQDs facilitated the charge transfer from the edge states of the GQDs to Hg^{2+} . On the other hand, the fast components (τ_1 and τ_2) were suggested to be related to intrinsic states of GQDs and decreased in the presence of melamine from 25.56% to 20.99% for τ_1 and from 55.05% to 41.30% for τ_2 , respectively. The Hg–melamine complex self-assembled on the surface of GQDs and melamine facilitated charge transfer from the intrinsic states of GQDs to Hg^{2+} . In the meantime, the slow component decreased to 37.70%, which might be attributed to the formation of the Hg–melamine complex and partial desorption of Hg^{2+} from the oxygen groups at the edge of the GQDs.

To better understand the melamine-induced quenching mechanism, we studied the influence of other substances with similar molecular structures on FL quenching. No obvious FL quenching was observed after adding 15 μM of thymine or uracil, but some FL quenching was observed after adding 15 μM of cytosine (Figure S4 in the Supporting Information). The distinctive FL quenching behavior of cytosine might be ascribed to its C=N bond, which is adjacent to an amino group, giving the molecule a conjugated structure. In contrast, neither thymine nor uracil has a conjugated structure, which is probably why neither of these materials induced FL quenching despite the fact that both have been proven to be among the most selective ligands for Hg^{2+} binding.^{38–40} Accordingly, both the functional groups (amine and triazine groups) and the π -conjugated structure of melamine played key roles in the quenching of GQDs: the former was responsible for coordination with Hg^{2+} , and the latter contributed to the assembly of the Hg–melamine complex on the surface of GQDs. As a strong chelating agent, ethylenediaminetetraacetic acid (EDTA) displayed a higher affinity for Hg^{2+} than for melamine. Thus we applied the reversible binding experiment to gain deeper insight into the role of Hg^{2+} . While the FL of GQDs was quenched in the presence of Hg^{2+} and melamine, the extra addition of 40 μM EDTA resulted in the recovery of FL emission (Figure S5 in the Supporting Information). This result could be ascribed to the desorption of Hg^{2+} from the surface of GQDs and the inhibition of the charge transfer from GQDs to Hg^{2+} .

Analytical Characteristics. This sensing system exhibited a rapid FL response: the FL quenching reached a stable value within 10 min after introducing Hg^{2+} and melamine (Figure S6

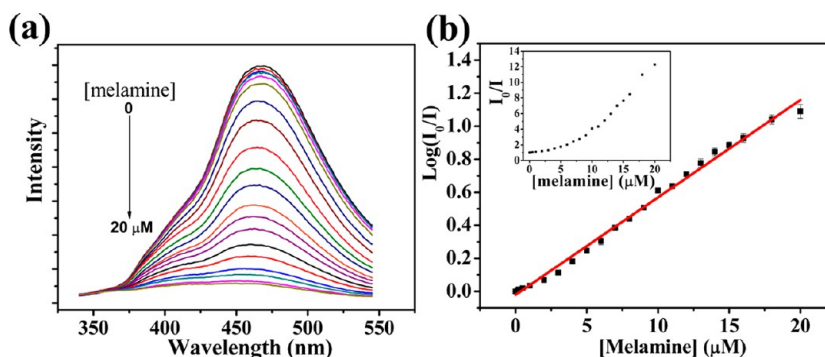


Figure 7. (a) FL quenching of GQDs containing Hg^{2+} (40 μM) in the presence of different concentrations of melamine. The concentrations of melamine were 0, 0.15, 0.20, 0.25, 0.50, 1.0, 2.0, 3.0, 4.0, 5.0, 6.0, 7.0, 8.0, 9.0, 10, 12, 14, 16, 18, and 20 μM , respectively. (b) The relationship between the sensor and [melamine]; inset is the Stern–Volmer plot. I and I_0 are FL intensity of GQDs- Hg^{2+} with and without melamine, respectively.

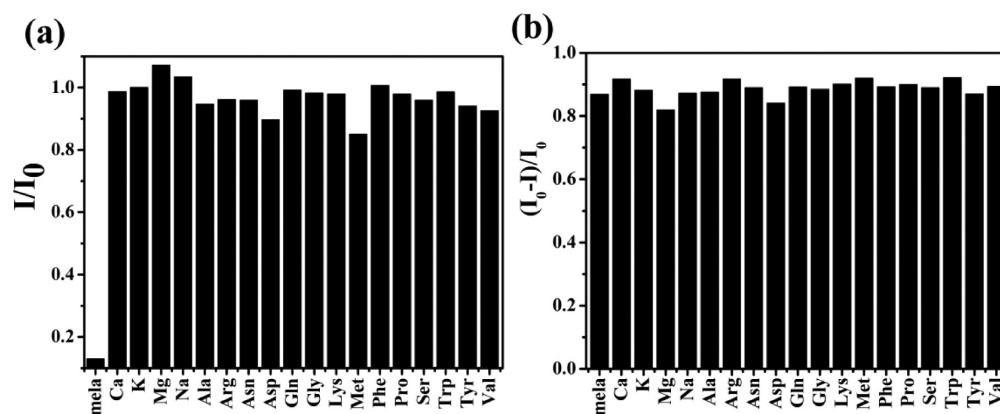


Figure 8. (a) Selectivity of the sensing system for melamine over amino acids. All substances were added to solution at a concentration of $15 \mu\text{M}$. The labels Ca, K, Mg, and Na represent Ca^{2+} , K^+ , Mg^{2+} , Na^+ , respectively. (b) FL response of the sensor to melamine in the presence of competitive substances. The concentration of melamine and of all competitive substances was $15 \mu\text{M}$.

in the Supporting Information). FL spectra of GQD solutions were recorded at 466 nm (ex: 285 nm) following incubation with Hg^{2+} and melamine for 10 min at room temperature.

Figure 7 presents the change in FL intensity of GQDs ($20 \mu\text{g mL}^{-1}$) containing Hg^{2+} ($40 \mu\text{M}$) in the presence of different concentrations of melamine. The Stern–Volmer plot of FL quenching was highly curved, while the logarithm of the FL intensity was proportional to melamine concentration in the range from 0.15 to $20 \mu\text{M}$ (0.019–2.5 ppm). The regression equation was $y = 0.05892x - 0.02029$, with a correlation coefficient (R^2) of 0.9942, where y and x are the logarithm of the FL intensity ratio and melamine concentration, respectively. The limit of detection was $0.12 \mu\text{M}$ (15 ppb) based on a signal-to-noise ratio of 3, which is comparable with other methods such as GC/MS (2 ppb) and SERS (0.1 ppm).^{20,41} This detection limit is far below the regulatory level of 2.5 ppm in the U.S. or 1 ppm in China for infant formula, suggesting the promising practical usage of this sensing system.

Selectivity. To evaluate the selectivity of the proposed sensor, the interference of some metal ions and fourteen amino acids that might be present in real samples was investigated (Figure 8a). The results showed that $15 \mu\text{M}$ concentrations of amino acids, even those with aromatic rings, had little influence on the FL intensity of the sensor. In addition, an experiment was carried out in which both $15 \mu\text{M}$ melamine and competitive substances were added (Figure 8b). The results revealed that the competitive substances had minor or no interference on the FL quenching response to melamine, indicating the high selectivity for melamine in the presence of these interfering substances.

Determination of Melamine in Raw Milk. To verify the performance of this sensor in real milk products, we prepared raw milk samples spiked with certain amounts of melamine. The practical samples were pretreated according to a general procedure, and the results were listed in Table 1. Sample recoveries, the ratios of the found concentration to the added

Table 1. Determination Results of Melamine in Raw Milk

samples	added (ppm)	found (ppm)	recovery (%)
1	0	0	
2	0.2	0.19	95
3	0.8	0.81	101
4	2.0	2.06	103

concentration, were in the range from 95% to 103%. Compared with other previous methods, this approach has comparable practicability and accuracy.^{20,21} Therefore, this sensor can be applied for melamine detection in real samples.

CONCLUSIONS

By making use of the sp^2 -bonded carbon lattice structure and the FL of GQDs, we have developed a novel type of rapid and sensitive GQDs-based sensor for the detection of melamine, relying on the fact that the Hg^{2+} in close proximity to the surface of GQDs could quench the FL of GQDs by means of charge transfer. This is the first reported method for melamine detection in which melamine acts as a linkage agent between the donor and the quencher. The rapid FL response of this sensing system makes it attractive for practical detection of melamine. This method allows a detection limit as low as 15 ppb, thus meeting regulatory requirements, and also exhibits advantages such as simple fabrication, convenient operation and high selectivity for melamine against interferences that may exist in real samples. Therefore, this method has great potential application for melamine detection in real samples. In view of the toxicity and environmental contamination of mercury, it's necessary to ensure proper disposal of mercury garbage and encourage procedures without the use of mercury.⁴² However, this design principle of FL quenching by charge transfer from GQDs to a metal ion coordinated with the target may be extended for detection of other molecules.

ASSOCIATED CONTENT

Supporting Information

Additional information as noted in text. This material is available free of charge via the Internet at <http://pubs.acs.org>.

AUTHOR INFORMATION

Corresponding Author

*Tel: +86 25 83594196. Fax: +86 2583594196. E-mail: jjzhu@nju.edu.cn.

Author Contributions

[§]L. L. and G. W. contributed equally to this work.

Notes

The authors declare no competing financial interest.

ACKNOWLEDGMENTS

We greatly appreciate the financial support from the National Basic Research Program of China (2011CB933502) and the support from the National Natural Science Foundation of China (21020102038, 21121091, 21175065). The authors extend their appreciation to the Deanship of Scientific Research at King Saud University for funding the work through the research group project (RGP-VPP-029).

REFERENCES

- (1) Li, Y.; Hu, Y.; Zhao, Y.; Shi, G.; Deng, L.; Hou, Y.; Qu, L. *Adv. Mater.* **2011**, *23*, 776–780.
- (2) Liu, R.; Wu, D.; Feng, X.; Müllen, K. *J. Am. Chem. Soc.* **2011**, *133*, 15221–15223.
- (3) Yan, X.; Cui, X.; Li, L.-s. *J. Am. Chem. Soc.* **2010**, *132*, 5944–5945.
- (4) Li, L.; Wu, G.; Yang, G.; Peng, J.; Zhao, J.; Zhu, J.-J. *Nanoscale* **2013**, *5*, 4015–4039.
- (5) Tang, L.; Ji, R.; Cao, X.; Lin, J.; Jiang, H.; Li, X.; Teng, K. S.; Luk, C. M.; Zeng, S.; Hao, J.; Lau, S. P. *ACS Nano* **2012**, *6*, 5102–5110.
- (6) Li, L.-L.; Ji, J.; Fei, R.; Wang, C.-Z.; Lu, Q.; Zhang, J.-R.; Jiang, L.-P.; Zhu, J.-J. *Adv. Funct. Mater.* **2012**, *22*, 2971–2979.
- (7) Lin, L.; Zhang, S. *Chem. Commun.* **2012**, *48*, 10177–10179.
- (8) Zhu, S.; Zhang, J.; Qiao, C.; Tang, S.; Li, Y.; Yuan, W.; Li, B.; Tian, L.; Liu, F.; Hu, R.; Gao, H.; Wei, H.; Zhang, H.; Sun, H.; Yang, B. *Chem. Commun.* **2011**, *47*, 6858–6860.
- (9) Zhuo, S.; Shao, M.; Lee, S.-T. *ACS Nano* **2012**, *6*, 1059–1064.
- (10) Dutta, M.; Sarkar, S.; Ghosh, T.; Basak, D. *J. Phys. Chem. C* **2012**, *116*, 20127–20131.
- (11) Peng, J.; Gao, W.; Gupta, B. K.; Liu, Z.; Romero-Aburto, R.; Ge, L.; Song, L.; Alemany, L. B.; Zhan, X.; Gao, G.; Vithayathil, S. A.; Kaiparettu, B. A.; Marti, A. A.; Hayashi, T.; Zhu, J.-J.; Ajayan, P. M. *Nano Lett.* **2012**, *12*, 844–849.
- (12) Sun, H.; Wu, L.; Gao, N.; Ren, J.; Qu, X. *ACS Appl. Mater. Inter.* **2013**, *5*, 1174–1179.
- (13) Zhu, S. J.; Zhang, J. H.; Tang, S. J.; Qiao, C. Y.; Wang, L.; Wang, H. Y.; Liu, X.; Li, B.; Li, Y. F.; Yu, W. L.; Wang, X. F.; Sun, H. C.; Yang, B. *Adv. Funct. Mater.* **2012**, *22*, 4732–4740.
- (14) Zhang, M.; Bai, L. L.; Shang, W. H.; Xie, W. J.; Ma, H.; Fu, Y. Y.; Fang, D. C.; Sun, H.; Fan, L. Z.; Han, M.; Liu, C. M.; Yang, S. H. *J. Mater. Chem.* **2012**, *22*, 7461–7467.
- (15) Dong, Y. Q.; Li, G. L.; Zhou, N. N.; Wang, R. X.; Chi, Y. W.; Chen, G. N. *Anal. Chem.* **2012**, *84*, 8378–8382.
- (16) Ran, X.; Sun, H.; Pu, F.; Ren, J.; Qu, X. *Chem. Commun.* **2013**, *49*, 1079–1081.
- (17) Bai, J.-M.; Zhang, L.; Liang, R.-P.; Qiu, J.-D. *Chem.—Eur. J.* **2013**, *19*, 3822–3826.
- (18) Chan, E. Y. Y.; Griffiths, S. M.; Chan, C. W. *Lancet* **2008**, *372*, 1444–1445.
- (19) Brown, C. A.; Jeong, K.-S.; Poppenga, R. H.; Puschner, B.; Miller, D. M.; Ellis, A. E.; Kang, K.-I.; Sum, S.; Cistola, A. M.; Brown, S. A. *J. Vet. Diagn. Invest.* **2007**, *19*, 525–531.
- (20) Miao, H.; Fan, S.; Wu, Y.-N.; Zhang, L.; Zhou, P.-P.; Li, J.-G.; Chen, H.-J.; Zhao, Y.-F. *Biomed. Environ. Sci.* **2009**, *22*, 87–94.
- (21) Zhu, H.; Zhang, S.; Li, M.; Shao, Y.; Zhu, Z. *Chem. Commun.* **2010**, *46*, 2259–2261.
- (22) Chen, L.-M.; Liu, Y.-N. *ACS Appl. Mater. Interfaces* **2011**, *3*, 3091–3096.
- (23) Garber, E. A. E. *J. Food Prot.* **2008**, *71*, 590–594.
- (24) Cao, Q.; Zhao, H.; He, Y.; Ding, N.; Wang, J. *Anal. Chim. Acta* **2010**, *675*, 24–28.
- (25) Ai, K.; Liu, Y.; Lu, L. *J. Am. Chem. Soc.* **2009**, *131*, 9496–9497.
- (26) Lee, J.; Jeong, E. J.; Kim, J. *Chem. Commun.* **2011**, *47*, 358–360.
- (27) Qi, W. J.; Wu, D.; Ling, J.; Huang, C. Z. *Chem. Commun.* **2010**, *46*, 4893–4895.
- (28) Attia, M. S.; Bakir, E.; Abdel-aziz, A. A.; Abdel-mottaleb, M. S. A. *Talanta* **2011**, *84*, 27–33.
- (29) Chakraborti, H.; Sinha, S.; Ghosh, S.; Pal, S. K. *Mater. Lett.* **2013**, *97*, 78–80.
- (30) Mei, Q.; Jiang, C.; Guan, G.; Zhang, K.; Liu, B.; Liu, R.; Zhang, Z. *Chem. Commun.* **2012**, *48*, 7468–7470.
- (31) Wiles, A. B.; Bozzuto, D.; Cahill, C. L.; Pike, R. D. *Polyhedron* **2006**, *25*, 776–782.
- (32) Hummers, W. S.; Offeman, R. E. *J. Am. Chem. Soc.* **1958**, *80*, 1339–1339.
- (33) Pan, D.; Zhang, J.; Li, Z.; Wu, M. *Adv. Mater.* **2010**, *22*, 734–738.
- (34) Fan, L. S.; Hu, Y. W.; Wang, X.; Zhang, L. L.; Li, F. H.; Han, D. X.; Li, Z. G.; Zhang, Q. X.; Wang, Z. X.; Niu, L. *Talanta* **2012**, *101*, 192–197.
- (35) Algar, W. R.; Tavares, A. J.; Krull, U. J. *Anal. Chim. Acta* **2010**, *673*, 1–25.
- (36) Chen, J.-L.; Yan, X.-P.; Meng, K.; Wang, S.-F. *Anal. Chem.* **2011**, *83*, 8787–8793.
- (37) Liu, F.; Jang, M.-H.; Ha, H. D.; Kim, J.-H.; Cho, Y.-H.; Seo, T. S. *Adv. Mater.* **2013**, *25*, 3657–3662.
- (38) Li, D.; Wieckowska, A.; Willner, I. *Angew. Chem. Int. Edit.* **2008**, *47*, 3927–3931.
- (39) Ye, B.-C.; Yin, B.-C. *Angew. Chem. Int. Edit.* **2008**, *47*, 8386–8389.
- (40) Ono, A.; Torigoe, H.; Tanaka, Y.; Okamoto, I. *Chem. Soc. Rev.* **2011**, *40*, 5855–5866.
- (41) Du, X.; Chu, H.; Huang, Y.; Zhao, Y. *Appl. Spectrosc.* **2010**, *64*, 781–785.
- (42) Zahir, F.; Rizwi, S. J.; Haq, S. K.; Khan, R. H. *Environ. Toxicol. Pharmacol.* **2005**, *20*, 351–360.